GA–A24043

CONTROL OF THE INJECTED RF BEAM IN THE DIII–D ECH SYSTEM

by
K. KAJIWARA, C.B. BAXI, J.L. DOANE, R.E. ELLIS, M.E. FRIEND,
M. GREEN, Y.A. GORELOV, J. LOHR, C.P. MOELLER, R.I. PINSKER,
D. PONCE, and R. PRATER

AUGUST 2002

DISCLAIMER

GA–A24043

CONTROL OF THE INJECTED RF BEAM IN THE DIII–D ECH SYSTEM

by

K. KAJIWARA,* C.B. BAXI, J.L. DOANE, R.E. ELLIS,† M.E. FRIEND, M. GREEN, Y.A. GORELOV, J. LOHR, C.P. MOELLER, R.I. PINSKER, D. PONCE, and R. PRATER

This is a preprint of a paper to be presented at the Twenty-Seventh International Conference on Infrared and Millimeter Waves, September 22–26, 2002, San Diego, California, and to be published in the *Proceedings*.

*Oak Ridge Instiutute for Science Education, Oak Ridge, Tennessee.
†Princeton Plasma Physics Laboratory, Princeton, New Jersey.

Work supported by
the U.S. Department of Energy under
Contract Nos. DE-AC03-99ER54463, DE-AC05-76OR00033,
and DE-AC02-76CH203073

GENERAL ATOMICS PROJECT 30033
AUGUST 2002

Thermal Performance of the Launcher Mirrors in the DIII–D ECH System

K. Kajiwara,[a] C.B. Baxi, R.W. Callis, J.L. Doane, R.L. Ellis,[b] M.E. Friend, M. Green, Y.A. Gorelov, J. Lohr, C.P. Moeller, R.I. Pinsker, D. Ponce, and R. Prater

General Atomics, P.O. Box 85608, San Diego, California 92186-5608

[a]Oak Ride Institute for Science Education, Oak Ridge, Tennessee.

[b]Princeton Plasma Physics Laboratory, Princeton NJ, USA

Abstract. The DIII-D ECH system includes three launcher assemblies each of which can accommodate the rf beams from two gyrotrons. The launchers use four different designs for the mirrors which focus and direct the beams into the tokamak. The designs use molybdenum brazed to graphite, thin Glidcop or variable thickness Glidcop. A fourth design with laminated Glidcop/stainless steel construction has been operated, but no thermal data are available. All the mirrors operate without active cooling. This paper presents preliminary analyses and measurements of the thermal performance of the three designs for which data have been obtained.

I. INTRODUCTION

The recent adaptation of diamond output windows, artificially grown using the Chemical Vapor Deposition (CVD) technique, has made possible the development of gyrotrons with high output power up to and greater than 1 MW, with long pulses approaching cw. CVD diamond has extremely high rf transparency near 100 GHz and thermal conductivity about four times greater than copper. This enables the gyrotrons to be designed for Gaussian output beams which couple well to the $HE_{1,1}$ fundamental circular waveguide mode, which propagates the rf with extremely low loss. For a 100 m transmission line with 14 miter bends, -1 dB loss has been measured. These developments all increase the requirements for thermal performance of the launcher system at the target. The launcher antennas, providing flexibility in steering and operating in vacuum, must be designed to withstand the extremely high power rf beams and the forces generated by the disruption of the plasma and can become the most highly stressed part of the system.

II. MIRROR DESIGNS

All of the DIII-D antennas include focus mirrors and flat steerable mirrors as shown in Fig. 1. Although the fixed focusing mirrors can be firmly mounted and are not susceptible to damage from disruption forces, the steerable mirrors have actuators, pivots and other delicate structures which can be damaged by magnetically derived torques. Magnetic forces can be reduced by reducing the inductively driven eddy currents generated during disruptions. This can be accomplished by increasing the resistivity of the mirrors, by reducing the amount of current carrying material, by increasing the path lengths for circulating currents, by properly orienting the conductors and by shielding. Each of these techniques presents practical difficulties that can adversely affect the rf performance of the mirrors. For example, decreasing the amount of material reduces the thermal inertia of the mirrors, which can result in unacceptable temperatures, while resistive materials make poor reflectors.

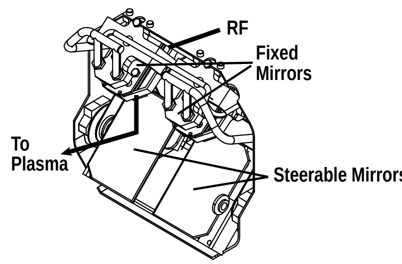

Fig. 1. The launchers have weekly focusing fixed mirrors and flat steering mirrors. Steering mirrors on two launchers can be scanned both poloidally and toroidally. The older design has fixed toroidal injection angle and poloidal scanning only. Each launcher assembly accommodates the rf beams from two gyrotrons.

The first mirrors for DIII-D launchers were made from pyrolytic graphite overcoated with a few microns of molybdenum with a thin copper surface vacuum evaporated onto the molybdenum. These mirrors had good radiation cooling and were nearly force-free during disruptions. However, the surfaces evolved gas during operation which led to rf arcs and surface etching.

A second set of mirrors [Fig. 2(a)] was made from relatively thin Glidcop, about 3.2 mm in thickness. These mirrors were calculated to withstand a 2 s, 800 kW rf beam without surface arcing or excessive heating. The large eddy currents associated with this design, ruled it out on mechanical grounds for fully articulating launchers, however. It also could not handle the large heat loads from 5–10 second duration rf beams. The design was modified [Fig. 2(b)] with the ddition of a boss, or thicker region on the back at the center to increase the thermal inertia with only modest increase in disruption forces, plus grooves and acid etching on the back to increase the radiative cooling. This mirror was calculated to be capable of 800 kW, 10 s operation with 15 minutes between pulses, or a 1% duty cycle. The design could be used for single axis steering mirrors with rugged mounts.

Two additional designs were developed by the Princeton Plasma Physics Laboratory (PPPL) for the two-axis PPPL articulating launchers built for DIII–D. In one design, the mirrors are made from graphite with a 0.38 mm thick molybdenum surface bonded to it by brazing [Fig. 2(c)]. This mirror design significantly reduces the eddy current loading and handles high temperatures well at the expense of increased rf losses due to the resistivity of the molybdenum. Owing to ratcheting of the temperature of this mirror, the pulse length is limited to 5 s in normal service. A second design consists of a copper and stainless steel laminate with a solid copper reflecting surface. The copper laminations carry heat away from the front surface, and provide thermal inertia while the stainless steel contributes sufficient strength to react to the increased disruption forces. In this design, the mechanical pivot structures had to be strengthened. Although a mirror with this design has been used in DIII-D, no thermal data are available.

II. COMPARISON BETWEEN SIMULATION AND MEASUREMENT

The mirror temperatures are measured by platinum resistance temperature devices (RTDs) attached to the mirrors. The time evolutions of the RTD measured temperatures are shown in Fig. 3(a,b,c) for the flatcopper mirror, the copper mirror with boss and the PPPL molybdenum/graphite mirrors, respectively. The rf pulse length was about 800 ms and the rf power at the mirrors was ~500 kW. During plasma discharges the RTDs are disconnected from the measurement system, therefore there is a gap in the record and the full time evolution during and just after the discharge is not obtained. As shown in Fig. 3, the temperature peaks within 200 s and then decreases slowly. Without an active cooling system, the temperature decrease occurs primarily due to radiative cooling. The temperatures for the flat and the bossed copper mirrors have about the same rise times. However, the graphite mirror more quickly reaches the highest temperature, showing the higher microwave absorption of molybdenum and lower heat capacity of graphite compared with Gildcop.

The peak temperature linearly increases as the pulse width increases (Fig. 4). The temperature increase of the copper boss mirror is lower than the flat mirror due to the higher thermal mass and the effectiveness of the measures taken to increase the radiative cooling by treating the back surface. The molybdenum/graphite mirrors reach the highest temperature. The data for pulse width zero in Fig. 4 indicate mirror heating due to the plasma alone without ECH injection. The points show that the contribution from the plasma is small compared with the rf heating in these experiments.

For the present case, the rf losses of the flat copper mirror, the copper mirror with boss and the PPPL mirror were expected to be about 0.29%, 0.23% and 0.38%, respectively. The best fits to the data are for 0.13% loss

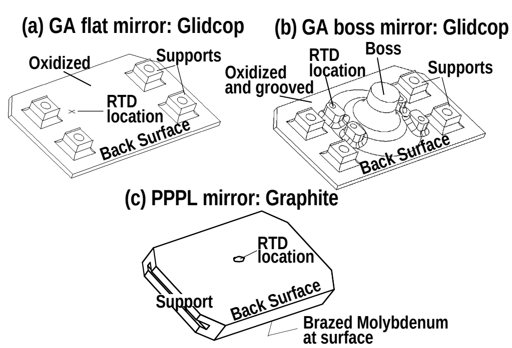

Fig. 2. The thermal performances of three different mirror designs are reported. (a) Flat Glidcop mirror with constant thickness except for mounting studs, (b) Glidcop mirror with a machined boss to increase the thermal mass with relatively low magnetic torques during disruptions, (c) graphite mirror with brazed molybdenum reflecting surface.

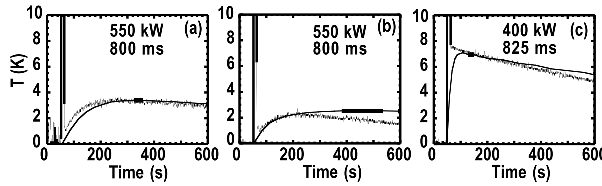

Fig. 3. Time dependence of the mirror temperature following a pulse into plasma. The measurement circuit is disconnected during the pulse. The solid curves are finite element model calculations using 0.13% Ohmic loss for copper and 0.32% for molybdenum. The rate of temperature decay after the pulse is greater than expected.

for the copper and 0.32% for molybdenum. With these losses and the free-space Gaussian beam profile launched from the open end of the waveguide as input, a 3-D thermal analysis was performed using the finite element code COSMOS. The radiation from the plasma was ignored in this calculation.

In every case the calculated peak temperatures, are higher than the experimental results. The calculations an be brought into agreement with the measurements, as indicated in Fig. 4, if 0.13% for copper and 0.32% for molybdenum rf loss is assumed. Under the assumption of this lower rf absorption, the time dependence of the temperature has been calculated and superimposed on the measurements as the bold lines in Fig. 3. Although the time dependence is in good agreement with the data during the heating, the measured temperature decreases more rapidly than indicated by the model.

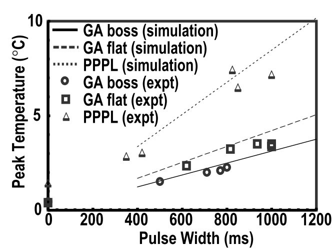

Fig. 4. The peak temperature is a linear function of pulse length. An Ohmic loss of 0.13% for copper and 0.32% for molybdenum is seen to represent the measurements well.

IV. CONCLUSION

The thermal performance of three different ECH launcher mirrors with different designs, all of which have passive radiative cooling, are measured. The peak temperatures increase linearly with pulse length. However, the peak temperatures are lower than the values predicted using electromagnetic theory and the decrease of temperature following the peak occurs faster than the prediction from finite element modeling. All the designs are adequate for the 800 kW, 5 s rf pulses currently being generated in the DIII-D experiment.

ACKNOWLEDGMENT

This work was supported by the U.S. Department of Energy under Contract Nos. DE-AC05-76OR00033, DE-AC03-99ER54463, and DE-AC02-76CH03073.